Materials Today: Proceedings xxx (xxxx) xxx

Contents lists available at ScienceDirect

Materials Today: Proceedings

journal homepage: www.elsevier.com/locate/matpr

Utilization of lamtoro fruit peel waste to improve the performance of supercapacitor electrodes in energy storage

Rika Taslim [a], Inri Br Pasaribu [b], Novi Yanti [b], Apriwandi Apriwandi [b], Erman Taer [b,*]

[a] Department of Industrial Engineering, Islamic State University Sultan Syarif Kasim Riau, Pekanbaru 28293, Indonesia
[b] Department of Physics, Faculty of Mathematics and Natural Sciences, University of Riau, Pekanbaru 28293, Indonesia

ARTICLE INFO

Article history:
Available online xxxx

Keywords:
Lamtoro fruit peel
Uncomplicated
Cost-effective
Activated carbon electrodes
Supercapacitor

ABSTRACT

This study aimed to prepare activated carbon obtained from biomass waste of lamtoro fruit peel, *Leucaena leucocephala (Lam.)* (LAC), and analyze its physical as well as electrochemical properties. The preparation process used a simple, uncomplicated, and cost-effective technique that does not require additional adhesive to increase the use value of biomass waste. Furthermore, impregnation with low $ZnCl_2$ concentrations at 0.1, 0.3, and 0.5 M was performed to maximize the potential of LAC to produce the best conditions from the electrode with the highest specific capacitance. The results showed that the LAC-0.3 sample had the best physical and electrochemical properties with the carbon content reaching 93.05 % and the availability of 6.89 % oxygen heteroatom doping. Besides, the large number of irregular porous lumps in the sample can increase the electrochemical performance of the carbon electrode from 74F/g to 176F/g, with an optimum energy density of 26.81 Wh kg^{-1} and a power density of 96.6 W kg^{-1} obtained using the GCD method. Electrochemical testing for LAC samples was carried out at a low potential of 0–1 V with a scan rate of 1 mV s^{-1} and an aqueous electrolyte of 1 M H_2SO_4. These findings showed the extraordinary potential of lamtoro fruit peel waste as a basic material for making activated carbon electrodes for supercapacitor with competitive capacitance.

1. Introduction

The imbalance between energy development and human needs has continued to raise the demand for constant improvements in energy storage devices and their conversion [1–3]. Energy resources such as sun, ocean waves, wind, and geothermal have been selected as alternatives, along with the depletion of fossil fuel energy availability [4]. These alternatives need high-capacity storage devices due to limited availability, such as solar energy running out at night as well as less wind when the weather is calm. Rechargeable high-energy storage devices, such as batteries and supercapacitor, have great potential in realizing efficient energy availability through electrochemical processes [5]. Although batteries have superior energy compared to supercapacitor, they are only suitable for single use, expensive to produce, and have a relatively short life cycle [6]. Supercapacitor is advanced energy storage devices with large specific capacitance, high power density, long cycle life, and environmentally friendly [7,8]. It can also be applied in various fields such as network stations, portable electronics, and transportation [9,10]. In general, a supercapacitor consists of two electrodes, a current collector, a charge/electrolyte source, and a separator [11,12]. Currently, increasing the energy density of supercapacitor while also maintaining its long life cycle and high power density is a great challenge [13,14]. The electrode component is a key factor in improving electrochemical performance [15]. Activated carbon, metal oxides, conductive polymers, or sulfide nanocomposites can be used as the base material for making electrodes in supercapacitor components [16]. Biomass-based activated carbon has the potential to improve the performance of commercial electrodes by continuously optimizing their conversion by adjustable pore structure. It also ensures a high surface area, availability of natural micropores, and is environmentally friendly [17]. Biomass carbon can be obtained from the remains of living things and processed through a series of heating to high temperatures [18]. Usually, the processing of biomass into

* Corresponding author.
E-mail address: erman.taer@lecturer.unri.ac.id (E. Taer).

https://doi.org/10.1016/j.matpr.2023.01.369

porous activated carbon is carried out by various methods such as hard/soft templating, hydrothermal, aerosol-assisted, and modified stöber [19]. Although these methods can produce porous carbon with a stronger and uniform pore structure, the workings and processing are complicated [20]. This study aims to process biomass waste into activated carbon with a simple, safe non-template technique, without harmful adhesives using simple fabrication tools [21].

Plant biomass waste was used as the base material for making porous carbon electrodes due to its abundant availability, high carbon content, rich natural micropores, and environmental friendliness [22–26]. Previous studies used green stem of cassava [26], corn silk [4], soybean stalks [27], and corn straw [28] as the basic ingredients for making porous activated carbon. In this study, the peel of the lamtoro fruit/petai china/Leucaena leucocephala (Lam.) was selected to manufacture an electrode material for supercapacitor cell components. The lamtoro plant is a type of small legume that can live in dry areas with poor soil conditions because it has a high nitrogen fixation ability. This plant can also act as a parasite because it contains the toxic chemical mimosine, as well as high carbon content with chemical compounds such as hemicellulose, cellulose, and lignin [29]. Usually, the leaves and twigs are used as a source of animal feed and firewood [29,30]. Based on this content, lamtoro fruit peel is expected to sufficiently produce porous activated carbon with a high purity level which can improve the performance of electrodes applied to supercapacitor. In addition, the fruit rind has not been studied as a base material for electrodes. The high carbon content produced was obtained through a combination method of chemical activation ($ZnCl_2$) and one-step integrated pyrolysis carbonization (N_2) with physical activation (CO_2). Varying concentrations of the chemical activator $ZnCl_2$, namely 0.1, 0.3, and 0.5 M, were used under the influence of 1 M H_2SO_4 aqueous electrolyte. This difference is expected to affect the performance of supercapacitor, while the overall process will reduce environmental pollution and increase the value of lamtoro fruit peel.

2. Materials and methods

The processing of biomass waste from lamtoro fruit peel into porous activated carbon for the basic material of electrode components in supercapacitor cells was carried out in several stages. This study was conducted based on the scope of synthesizing carbon nanotechnology materials. The detailed process of making activated carbon LAC is shown in Fig. 1.

The chemical zinc chloride ($ZnCl_2$) with different concentrations of 0.1, 0.3, and 0.5 M was used as a chemical activator to optimize the electrochemical performance of supercapacitor, while an electrolyte solution of sulfuric acid (H_2SO_4) 1 M was utilized as a source of charged ions during the electrochemical process. Moreover, aquades and pH indicators were used as neutralizing agents and for measuring the acidity of carbon materials. The important tools used include oven, ball milling grinder, 60 μm sieve, hot plate set, hydraulic press, and furnace. Based on Fig. 1, the process of making activated carbon for supercapacitor cell electrodes began with collecting the basic ingredients of lamtoro fruit peel waste from community plantations in the Rengat area, Indragiri Hulu Regency, Riau. A total of 3 kg samples were cut to a size of 3–5 cm to facilitate the drying process, then drying was carried out in the sun for 3 days, followed by using an oven at 110 °C for 48 h to reduce the moisture content. Drying was carried out until the sample mass loss was below 6 %, while pre-carbonization was conducted at a temperature range of 50–250 °C for 2.5 h using a vacuum oven by preparing a sample of 30 g, which was then put into a stainless-steel tube. The initial temperature of the oven was set at 50 °C, and increased by 50 °C to 250 °C every 30 min, thereby making the sample more brittle and turn the colour dark brown. Furthermore, a mortar was used to mash the sample to a millimeter scale, and re-mashing was carried out using ball milling to produce micro-sized particles. The working principle of ball milling is to utilize the collision between steel balls in a vacuum tube for 20 h. After a complete ball milling, it was sieved using a 60 μm sieve with the aid of a brush to obtain samples with < 60 μm carbon particles followed by activation using the addition of 0.1 M, 0.3 M and 0.5 M $ZnCl_2$ chemicals to observe the effect of the activator on the electrode capacity. The chemical activation process was carried out at a constant temperature of 80 °C with a stirring speed of 300 rpm to homogenize the sample. The samples were printed using a press with a mass of up to 8 tons to compact the carbon, while the pyrolysis process was performed in a one-step integrated system. The carbonization was initiated at room temperature up to 600 °C with N_2 gas absorption, followed by physical activation up to 800 °C under the influence of CO_2 gas. Subsequently, the samples were neutralized using the immersion method in 1 L of distilled water and dried again in an oven at a constant temperature of 110 °C for 2 days. Samples of dry carbon coins were polished to characterize their electrochemical properties.

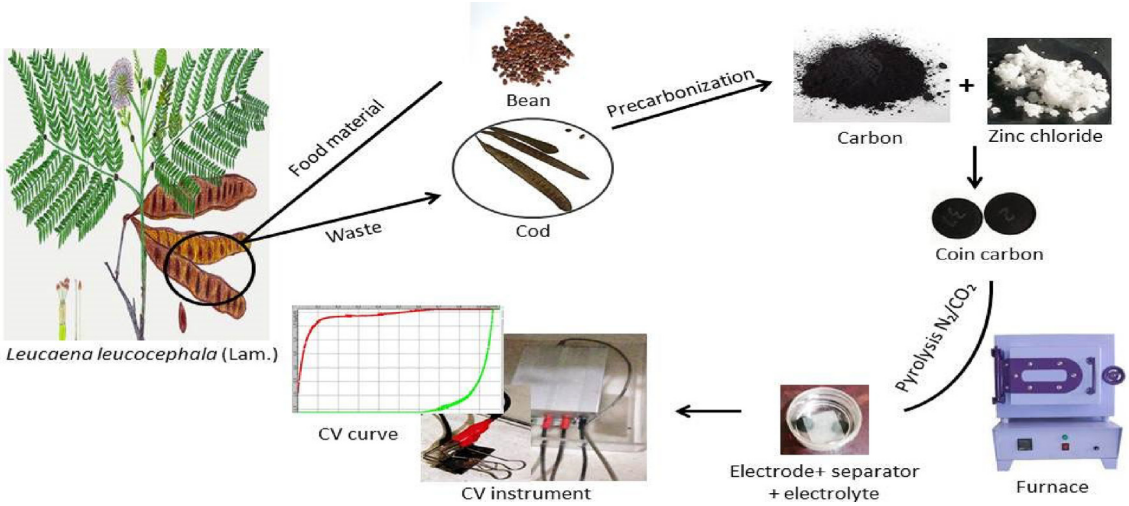

Fig. 1. Schematic of prepared activated carbon electrodes using lamtoro fruit peel waste for supercapacitor cell components.

The characterization was carried out by testing the physical and electrochemical properties of the activated carbon electrode. Physical properties were characterized by analyzing the density of carbon coins before and after pyrolysis, X-ray diffraction (XRD), electrode surface structure analysis (SEM) and constituent content analysis (EDS). Meanwhile, the electrochemical characterization was reviewed through two methods, namely cyclic voltammetry (CV) and galvanostatic charge–discharge (GCD). The test was carried out at a low potential window of 0 to 1 V, under the influence of an aqueous electrolyte of 1 M H_2SO_4 for each sample with different concentrations of activator ($ZnCl_2$) at 0.1, 0.3 and 0.5 M.

3. Results and discussions

LAC electrode density for all variations decreased significantly, and based on Fig. 2, the three variations that were affected by differences in the concentration of the chemical activator $ZnCl_2$ with sample codes LAC-0.1, LAC-0.3, and LAC-0.5 experienced significant shrinkage after passing through a single-stage integrated pyrolysis process. This result is in accordance with the density reduction data obtained in previous studies focused on making activated carbon using different biomass such as tofu dregs [31], and *Averrhoa bilimbi* leaves [32]. This shrinkage is presumably caused by several factors such as different concentrations of chemical activator $ZnCl_2$, carbonization, and physical activation [33]. Furthermore, the carbonization process can remove volatile elements that act as impurities in the carbon sample through evaporation, culminating in a porous structure [34]. The physical activation process at a temperature of 600 °C to 800 °C can remove impurities that cover the pores and improve the structure [35]. The addition of chemical activator $ZnCl_2$ with a low concentration of 0.1 M did not maximize the evaporation of elements other than carbon contained in the sample.

As shown in Table 1, sample LAC-0.1 experienced a density reduction of 16.5 % from its initial state, indicating that it does not have good porosity with low carbon purity, and cannot be used to optimize the performance of the electrode during the electrochemical working process. The addition of 0.3 M $ZnCl_2$ chemical activator concentration in the LAC-0.3 sample caused a reduction in the density of lamtoro fruit peel carbon by 31.2 %. At this concentration, maximum evaporation of elements other than carbon occurred, culminating in the production of porous carbon with good porosity, which can improve the performance of the electrode by providing rich active sites between the electrode and the electrolyte during electrochemical work. This condition can also optimize the absorption capacity to produce a higher specific surface area of activated carbon. Evaporation of elements other than carbon such as moisture, water, gas, and other volatile substances will facilitate the production of different pore structures in activated carbon samples [34]. The formation of this pore structure is expected to increase the absorption of ions by the electrode. Meanwhile, the addition of $ZnCl_2$ activator concentration up to 0.5 M in the sample caused the evaporation of carbon elements. Excessive evaporation of the LAC-0.5 sample can increase the pore size of the carbon and density due to the addition of $ZnCl_2$ activator concentration. Based on Table 1, the percentage decrease in density reached 20.6 % from the initial state. Therefore, the performance of the electrodes produced from the LAC-0.5 sample is not optimal.

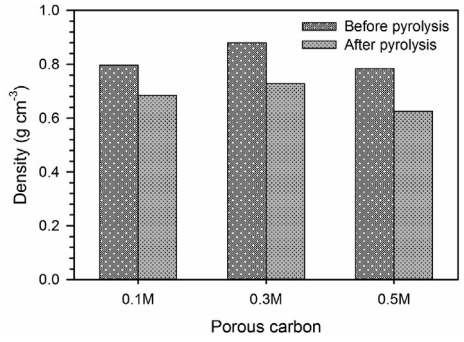

Fig. 2. Density shrinkage of samples LAC-0.1, LAC-0.3, and LAC-0.5 before and after pyrolysis.

XRD analysis for variations LAC-0.3 and LAC-0.5 displayed two diffraction peaks confirming the amorphous structure of the carbon samples in Fig. 3. The amorphous structure was confirmed at two sloping peaks, located in the (002) and (100) lattice planes respectively at 22–25 and 42-45° angles. The diffraction pattern of the LAC-0.3 sample had a wider peak intensity than LAC-0.5. This confirms the presence of an amorphous carbon structure with irregular pores associated with a rich microporosity [36] as an active site between the electrode and the charged electrolyte in the carbon matrix during the electrochemical work. Further evaluation results of the spacing between the microcrystalline layers and dimensions of the samples LAC-0.3 and LAC-0.5 are presented in Table 2. Meanwhile, these parameters were calculated based on Bragg's Law and the Debye-Scherer equation. The diffraction angles 002 and 100 which confirmed the amorphous structure of the samples experienced a slight shift due to the addition of the $ZnCl_2$ activator. Significantly small values of d_{002} and d_{100} indicate normal conditions for activated carbon samples based on nanoparticle materials. The value of d_{002} indicates the structure of graphite and d_{100} confirms the normal value for biomass-based carbon [37]. Furthermore, the height of the L_c microcrystalline layer is related to the microporosity structure of the carbon sample. The smaller Lc value of the sample LAC-0.3 confirms the availability of higher microporosity in increasing the surface area and porosity of the carbon material. According to Kumar (1997), these results are in accordance with the increase in the specific capacitance of the LAC-0.7 sample because the smaller the microcrystalline layer height, the larger the surface area with rich micropores. These data support the improvement of the electrochemical performance of the sample LAC-0.3 in the cyclic voltammetric test.

Further analysis regarding the content of activated carbon electrodes obtained from lamtoro fruit peel waste prepared by giving $ZnCl_2$ activator with different concentrations of 0.3 M and 0.5 M is detailed in Table 3. The LAC-0.3 sample demonstrated a higher level of purity with a carbon percentage reaching 93.05 % and an oxygen heteroatom doping of 6.89 %. The availability of self-doping oxygen heteroatoms in the sample contributes to specific capacitance by increasing the wettability of the carbon material and presenting pseudocapacitance properties that can cause current surges during the electrochemical performance process. Meanwhile, the addition of the activator concentration in the LAC-0.5 sample caused a decrease in the carbon content to 91.08 % and present crystalline impurities such as chlorine and calcium in small amounts, namely < 1 %. The decrease in carbon content was due to the reaction of the $ZnCl_2$ activating agent with the carbon and the high activation temperature setting which caused rapid gasification indicated by carbon evaporation. The addition of $ZnCl_2$ activator concentration can also lead to the presence of excess chlorine from the pyrolysis process, and calcium from the natural content of biomass. The EDS results are in accordance with previous studies that used different biomass such as citronella leaf waste [38] and wheat husk [39] with carbon percentages of 90.38 % and 87.96 %, respectively.

As shown in Fig. 4 a-d, the SEM morphology of the activated carbon obtained from lamtoro fruit peel biomass waste using 0.3 M and 0.5 M $ZnCl_2$ activator demonstrated a structure in the form of large irregular porous lumps. This appearance corresponds

Table 1
Percentage of density shrinkage before-after pyrolysis for each variation of LAC samples.

Sample	ρ_a(g cm^{-3})	ρ_b(g cm^{-3})	ρ(%)	Error measurement
LAC-0.1	0.84323	0.703742	16.5	0.019
LAC-0.3	0.906256	0.623209	31.2	0.022
LAC-0.5	0.846448	0.672093	20.6	0.009

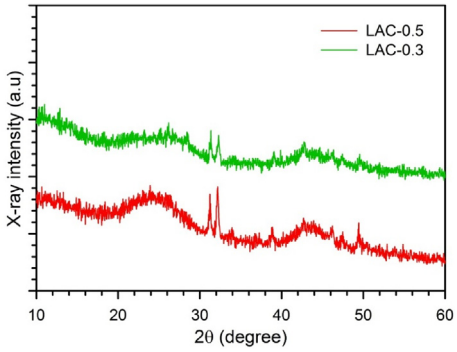

Fig. 3. XRD pattern for samples LAC-0.3 and LAC-0.5.

to the XRD pattern which shows the amorphous nature of the two LAC samples. The structure is produced through one-step integrated pyrolysis with carbonization of N_2 gas and physical activation of CO_2 gas up to a temperature of 800 °C which causes gasification of volatile compounds in carbon samples [40]. Using the IC Measure software, the pore size of the activated carbon formed was in the range of *meso* and macro pore sizes. The LAC-0.3 sample displayed morphology with a smaller lump size in greater numbers than LAC-0.5 with a random arrangement. The size of these pore particles ranged in the *meso* and macropores scales because of the particle structure in the form of lumps. This was confirmed in the LAC-0.3 sample with pores morphology in the form of large aggregates with a size range of 42–1121 nm. In addition, there are several pores such as nano-rod with a size of 53 nm and a pore distance between particles of 407 nm. As for the LAC-0.5 sample, it had fewer lumps and a larger size range, namely 202–1274 nm. This morphology makes LAC-0.3 superior with its relatively close pore spacing, which provides a shorter ion diffusion path in the electrochemical process. Consequently, this sample can be used to improve and optimize the performance of the supercapacitor with a higher specific capacitance than the other two samples. The pore morphology appearance of biomass-based activated carbon such as chunks was also found for the basic ingredients of pandanus thorn [41] and yam stem [37] in previous studies.

The electrochemical properties of activated carbon supercapacitor were measured using the Cyclic Voltammetry (CV) method to determine the specific capacitance value of each variation of the carbon electrode with the Physics CV UR Rad-ER 6481 tool. This measurement produces an output in the form of a distorted rectangular curve that characterizes a normal EDLC supercapacitor for biomass materials [42]. In this test, the carbon electrode of the lamtoro fruit peel was tested with aqueous electrolyte of 1 M H_2SO_4. The CV curve for activated carbon with $ZnCl_2$ concentrations of 0.1, 0.3 and 0.5 M is shown in Fig. 5a. These results indicated that the best electrode performance was produced by LAC-0.3 which had the widest CV curve and the highest specific capacitance value. This is because the addition of 0.3 M $ZnCl_2$ activator concentration in the carbon sample produced optimum conditions that can improve the performance of the supercapacitor electrode. Moreover, this condition is supported by the density and XRD measurement data of the sample which had the largest mass shrinkage and a small high value of the microcrystalline layer. This ensures the availability of rich micropores in the LAC-0.3 sample by providing an active site between the electrode and the electrolyte suitable for increasing the energy stored at the electrode.

Fig. 5b shows the relationship between specific capacitance and scan rates of 1, 2, 5 and 10 mV s^{-1} at a potential of 0 to 1 V. These results showed a wider CV curve for each sample variation at a test rate of 1 mV/s, indicating that the low scanning rate of 1 mV s^{-1} is the optimum ion speed to completely fill the electrode pores. The success of ion diffusion to fill the carbon pores causes an increase in the performance and ability of the lamtoro fruit peel carbon electrode by storing the highest electrochemical energy [43]. Furthermore, the graph shows the quantitative value of the specific capacitance of the carbon electrode with 0.1, 0.3, and 0.5 M $ZnCl_2$ activator under the influence of 1 M H_2SO_4 electrolyte. The specific capacitance values obtained can be compared with the results of previous studies that used different biomass with the same activator, as shown in Table 4.

The analysis of electrochemical properties was strengthened by measuring the Galvanostatic Charge Discharge (GCD) method using the CD UR Red-ER 2018 device with a constant current of 1 A. The electrochemical properties were evaluated in a two-electrode system under the influence of the same aqueous electrolyte, namely 1 M H_2SO_4. The results showed the relationship between voltage and time during the charging and discharging process, with the shape of the curve in the form of a distorted isosceles triangle, as shown in Fig. 6. This implies that the charge time has a big role in confirming the optimization of the specific capacitance value. GCD measurements were carried out in a potential voltage range of 0 V to 1 V with a constant current of 1 mA and a scan rate of 1 mV/s. The difference in time during the charge–discharge process is a factor that can affect the symmetry of the measurement curve [50]. LAC-0.3 had a longer measurement time than LAC-0.1 and LAC-0.5 as demonstrated by a larger isosceles triangle curve, indicating excellent electrochemical properties. The following table and values of specific capacitance, as well as energy and power densities are presented for each concentration variation of the lamtoro fruit peel electrode.

Based on Table 5, the highest specific capacitance and optimum conditions were found in the LAC-0.3 sample. This is because there

Table 2
Interlayer spacing and microcrystalline dimensions of samples LAC-0.3 and LAC-0.5.

Samples	$2\theta_{002}$ (°)	$2\theta_{100}$ (°)	d_{002} (Å)	d_{100} (Å)	L_c (Å)	L_a (Å)
LAC-0.3	24.992	42.622	3.56	2.119	15.375	18.760
LAC-0.5	25.799	44.835	3.45	2.019	10.869	26.822

Table 3
Status of elements on the surface of samples LAC-0.3 and LAC-0.5.

Samples	Chemical contain in activated carbon of lamtoro fruit peel (%)				
	Carbon	Oxygen	Magnesium	Clor	Calcium
LAC-0.3	93.05	6.89	0.06	0.00	0.00
LAC-0.5	91.08	6.18	0.55	0.34	1.86

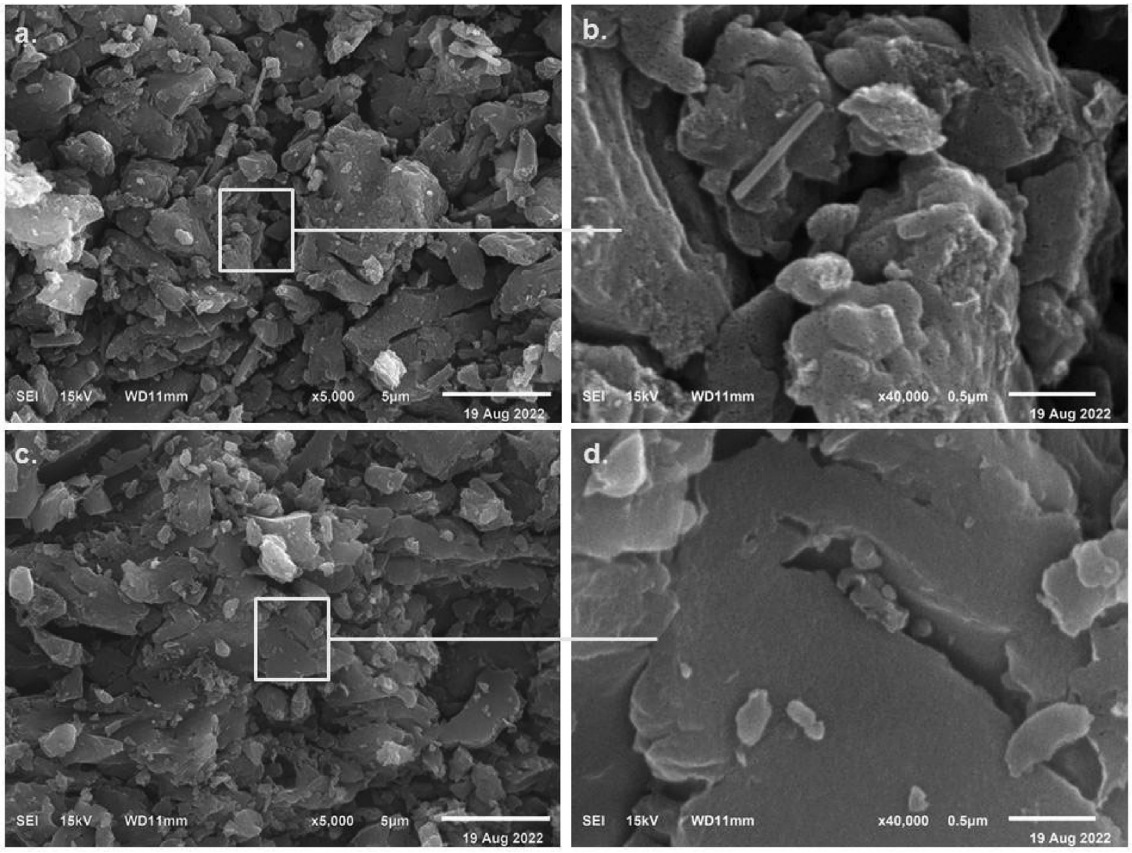

Fig. 4. Morphological structure display for samples LAC-0.3 and LAC-0.5.

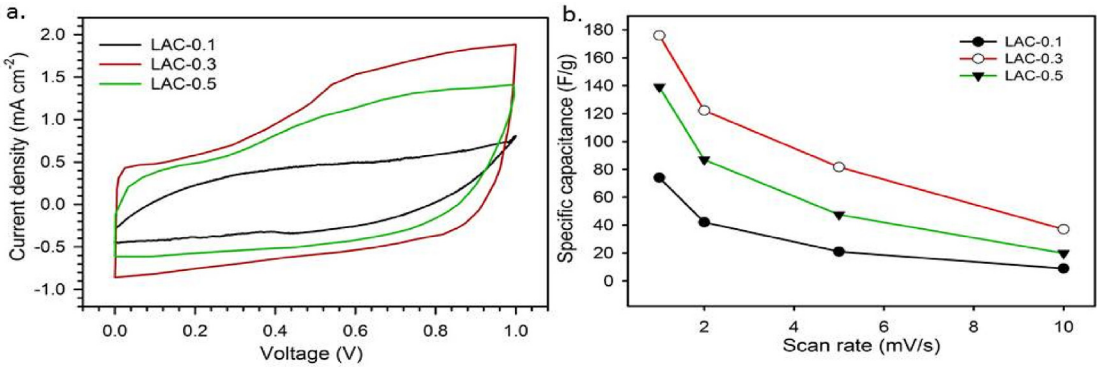

Fig. 5. A. cv curve of lac porous carbon for all concentration variations in 1 M H_2SO_4 at a scan rate of 1 mVs^{-1}b. Specific capacitance at scanning speed 1–10 mV s^{-1}.

is sufficient time for the ions to diffuse to fill the electrode pores during measurement and increase the specific capacitance value. Discharging time significantly influences the performance of supercapacitor electrodes [51]. A significant decrease during the discharge process is caused by the smaller pore radius, which interferes with the electrolyte ion transport process. Therefore, it takes time for the electrolyte ions to reach the surface of the activated carbon electrode. The GCD test results are in accordance with the CV test where the LAC-0.3 sample also produced a higher capacitance value than LAC-0.1 and LAC-0.5. This is also supported by data on density shrinkage, XRD, and testing of electrochemical properties using the CV method.

Table 4
Comparison of specific capacitance values of different biomass.

Biomass	Activator	C_{sp} (F/g)	Ref
Banana leaf	KOH	245	[44]
Soybean stalk	KOH	325	[27]
Tofu dregs	$ZnCl_2$	148	[31]
Chitin	$ZnCl_2$	277.4	[45]
Tobacco stalks	$ZnCl_2$	342	[46]
Oleana leaves	KOH	188	[47]
Banana stem waste	KOH	104.2	[48]
Bamboo stem	KOH	168.8	[49]
Lamtoro fruit skin	$ZnCl_2$	176	Research Now

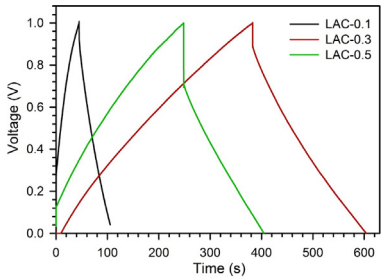

Fig. 6. GCD Graph of lamtoro fruit peel carbon electrodes for all variations of $ZnCl_2$ activator concentrations.

Table 5
Specific capacitance, energy, and power values of lamtoro fruit peel carbon electrodes based on the GCD Test.

Samples	C_{sp} (Fg^{-1})	E (Wh kg^{-1})	P (W kg^{-1})	Average error measurement (%)
LAC-0.1	81	11.25	40.54	4.6
LAC-0.3	193	26.81	96.6	3.8
LAC-0.5	157	21.81	78.58	7.2

4. Conclusions

The biomass waste of lamtoro fruit peel was successfully processed into porous activated carbon for supercapacitor electrodes. The processing is not complicated and is cost-effective because it does not require additional adhesive to increase the use value of biomass waste. Furthermore, variations in the concentration of the $ZnCl_2$ activator at 0.1, 0.3, and 0.5 M were used to obtain the best condition of the electrode with the highest specific capacitance. The chemical activation of $ZnCl_2$ in single-stage integrated pyrolysis was confirmed to increase the electrical charge storage capacity. Electrochemical properties were tested on a symmetrical two-electrode system with 1 M H_2SO_4 electrolyte at a voltage of 0–1 V and various scanning rates of 1, 2, 5 and 10 mV s^{-1}. The difference in the activator concentration used increased the electrochemical ability from 74F/g to 176F/g for the best electrode namely LAC-0.3. Further calculations of the improved electrochemical performance confirmed energy and power densities of 26.81 Wh kg^{-1} and 96.6 W kg^{-1}, respectively. These results supported the high potential of lamtoro fruit peel-based carbon electrodes to improve the energy storage performance of electrochemical supercapacitor.

CRediT authorship contribution statement

Rika Taslim: Visualization, Validation. **Inri Br Pasaribu:** Resources. **Novi Yanti:** Formal analysis, Writing – original draft. **Apriwandi Apriwandi:** Data curation, Writing – review & editing. **Erman Taer:** Conceptualization, Methodology.

Data availability

Data will be made available on request.

Declaration of Competing Interest

The authors declare that they have no known competing financial interests or personal relationships that could have appeared to influence the work reported in this paper.

Acknowledgements

The research was supported by second year Project of Word Class Research (WCR) in *Kementerian pendidikan, Kebudayaan, Riset, dan Teknologi*, Republic of Indonesia with contract No: 1627/UN19.5.1.3/PT.01.03/2022. Project title: "*Superkapasitor dengan Rapat Energi dan Daya Tinggi: Optimalisasi Proses Penyediaan Elektroda*".

References

[1] C. Zequine, C.K. Ranaweera, Z. Wang, S. Singh, P. Tripathi, O.N. Srivastava, B.K. Gupta, K. Ramasamy, P.K. Kahol, P.R. Dvornic, R.K. Gupta, High per formance and flexible supercapacitors based on carbonized bamboo fibers for wide temperature applications, Sci. Rep. 6 (2016) 1–10, https://doi.org/10.1038/srep31704.
[2] Z. Shang, X. An, L. Liu, J. Yang, W. Zhang, H. Dai, H. Cao, Q. Xu, H. Liu, Y. Ni, Chitin nanofibers as versatile bio-templates of zeolitic imidazolate frameworks for N-doped hierarchically porous carbon electrodes for supercapacitor, Carbohydr. Polym. 251 (2021), https://doi.org/10.1016/j.carbpol.2020.117107.
[3] Y. Gu, L.Q. Fan, J.L. Huang, C.L. Geng, J.M. Lin, M.L. Huang, Y.F. Huang, J.H. Wu, N-doped reduced graphene oxide decorated NiSe2 nanoparticles for high-performance asymmetric supercapacitors, J. Power Sources. 425 (2019) 60–68, https://doi.org/10.1016/j.jpowsour.2019.03.123.
[4] J. Zhou, S. Yuan, C. Lu, M. Yang, Y. Song, Hierarchical porous carbon microtubes derived from corn silks for supercapacitors electrode materials, J. Electroanal. Chem. 878 (2020), https://doi.org/10.1016/j.jelechem.2020.114704.
[5] K. Müller, Technologies for the Storage of Hydrogen. Part 2: Irreversible Conversion and Comparison, ChemBioEng Rev. 6 (2019) 81–89, https://doi.org/10.1002/cben.201900010.
[6] J. Büngeler, E. Cattaneo, B. Riegel, D.U. Sauer, Advantages in energy efficiency of flooded lead-acid batteries when using partial state of charge operation, J. Power Sources. 375 (2018) 53–58, https://doi.org/10.1016/j.jpowsour.2017.11.050.
[7] Y. Ma, M. Chen, X. Zheng, D. Yu, X. Dong, Synergetic effect of swelling and chemical blowing to develop peach gum derived nitrogen-doped porous carbon nanosheets for symmetric supercapacitors, J. Taiwan Inst. Chem. Eng. 101 (2019) 24–30, https://doi.org/10.1016/j.jtice.2019.04.031.
[8] E. Taer, K. Natalia, A. Apriwandi, R. Taslim, A. Agustino, R. Farma, The synthesis of activated carbon nanofiber electrode made from acacia leaves (Acacia mangium wild) as supercapacitors, Adv. Nat. Sci. Nanosci. Nanotechnol. 11 (2020), https://doi.org/10.1088/2043-6254/ab8b60.
[9] M. Vinayagam, R. Suresh Babu, A. Sivasamy, A.L. Ferreira de Barros, Biomass-derived porous activated carbon from Syzygium cumini fruit shells and Chrysopogon zizanioides roots for high-energy density symmetric supercapacitors, Biomass and Bioenergy. 143 (2020), https://doi.org/10.1016/j.biombioe.2020.105838.
[10] Y. Yoon, M. Lee, S.K. Kim, G. Bae, W. Song, S. Myung, J. Lim, S.S. Lee, T. Zyung, K. S. An, A Strategy for Synthesis of Carbon Nitride Induced Chemically Doped 2D MXene for High-Performance Supercapacitor Electrodes, Adv. Energy Mater. 8 (2018) 1–11, https://doi.org/10.1002/aenm.201703173.
[11] C. Zhong, Y. Deng, W. Hu, J. Qiao, L. Zhang, J. Zhang, A review of electrolyte materials and compositions for electrochemical supercapacitors, Chem. Soc. Rev. 44 (2015) 7484–7539, https://doi.org/10.1039/c5cs00303b.
[12] G. Lota, P. Krawczyk, K. Lota, A. Sierczyńska, Ł. Kolanowski, M. Baraniak, T. Buchwald, The application of activated carbon modified by ozone treatment for energy storage, J. Solid State Electrochem. 20 (2016) 2857–2864, https://doi.org/10.1007/s10008-016-3293-5.
[13] J.N. Caguiat, G. Arpino, S.G. Krigstin, D.W. Kirk, C.Q. Jia, Dependence of supercapacitor performance on macro-structure of monolithic biochar electrodes, Biomass and Bioenergy. 118 (2018) 126–132, https://doi.org/10.1016/j.biombioe.2018.08.017.
[14] C.J. Zhang, M.P. Kremer, A. Seral-Ascaso, S.H. Park, N. McEvoy, B. Anasori, Y. Gogotsi, V. Nicolosi, Stamping of Flexible, Coplanar Micro-Supercapacitors Using MXene Inks, Adv. Funct. Mater. 28 (2018) 1–10, https://doi.org/10.1002/adfm.201705506.

[15] J. Zhou, Y. Huang, X. Cao, B. Ouyang, W. Sun, C. Tan, Y. Zhang, Q. Ma, S. Liang, Q. Yan, H. Zhang, Two-dimensional NiCo2O4 nanosheet-coated three-dimensional graphene networks for high-rate, long-cycle-life supercapacitors, Nanoscale. 7 (2015) 7035–7039, https://doi.org/10.1039/c4nr06527a.
[16] Q. Jiang, N. Kurra, M. Alhabeb, Y. Gogotsi, H.N. Alshareef, All Pseudocapacitive MXene-RuO2 Asymmetric Supercapacitors, Adv. Energy Mater. 8 (2018) 1–10, https://doi.org/10.1002/aenm.201703043.
[17] W. Zhang, N. Lin, D. Liu, J. Xu, J. Sha, J. Yin, X. Tan, H. Yang, H. Lu, H. Lin, Direct carbonization of rice husk to prepare porous carbon for supercapacitor applications, Energy. 128 (2017) 618–625, https://doi.org/10.1016/j.energy.2017.04.065.
[18] D. He, Y. Gao, Z. Wang, Y. Yao, L. Wu, J. Zhang, Z.H. Huang, M.X. Wang, One-step green fabrication of hierarchically porous hollow carbon nanospheres (HCNSs) from raw biomass: Formation mechanisms and supercapacitor applications, J. Colloid Interface Sci. 581 (2021) 238–250, https://doi.org/10.1016/j.jcis.2020.07.118.
[19] M. Xu, Q. Yu, Z. Liu, J. Lv, S. Lian, B. Hu, L. Mai, L. Zhou, Tailoring porous carbon spheres for supercapacitors, Nanoscale. 10 (2018) 21604–21616, https://doi.org/10.1039/c8nr07560c.
[20] Y. Wang, Y. Song, Y. Xia, Electrochemical capacitors: Mechanism, materials, systems, characterization and applications, Chem. Soc. Rev. 45 (2016) 5925–5950, https://doi.org/10.1039/c5cs00580a.
[21] F. Xu, Z. Tang, S. Huang, L. Chen, Y. Liang, W. Mai, H. Zhong, R. Fu, D. Wu, Facile synthesis of ultrahigh-surface-area hollow carbon nanospheres for enhanced adsorption and energy storage, Nat. Commun. 6 (2015), https://doi.org/10.1038/ncomms8221.
[22] Q. Wang, M. Zhou, Y. Zhang, M. Liu, W. Xiong, S. Liu, Large surface area porous carbon materials synthesized by direct carbonization of banana peel and citrate salts for use as high-performance supercapacitors, J. Mater. Sci. Mater. Electron. 29 (2018) 4294–4300, https://doi.org/10.1007/s10854-017-8376-2.
[23] Z. Bi, Q. Kong, Y. Cao, G. Sun, F. Su, X. Wei, X. Li, A. Ahmad, L. Xie, C.M. Chen, Biomass-derived porous carbon materials with different dimensions for supercapacitor electrodes: A review, J. Mater. Chem. A. 7 (2019) 16028–16045, https://doi.org/10.1039/c9ta04436a.
[24] Y. Li, D. Zhang, Y. Zhang, J. He, Y. Wang, K. Wang, Y. Xu, H. Li, Y. Wang, Biomass-derived microporous carbon with large micropore size for high-performance supercapacitors, J. Power Sources. 448 (2020), https://doi.org/10.1016/j.jpowsour.2019.227396.
[25] M.A. Islam, H.L. Ong, A.R. Villagracia, K.A. Khairul, A.B. Ganganboina, R.A. Doong, Biomass–derived cellulose nanofibrils membrane from rice straw as sustainable separator for high performance supercapacitor, Ind. Crops Prod. 170 (2021), https://doi.org/10.1016/j.indcrop.2021.113694.
[26] E. Taer, N. Yanti, W.S. Mustika, A. Apriwandi, R. Taslim, A. Agustino, Porous activated carbon monolith with nanosheet/nanofiber structure derived from the green stem of cassava for supercapacitor application, Int. J. Energy Res. 44 (2020) 10192–10205, https://doi.org/10.1002/er.5639.
[27] Y. Zhao, R. Xu, J. Cao, X. Zhang, J. Zhu, X. Wei, N / O co-doped interlinked porous carbon nano fl akes derived from soybean stalk for high-performance supercapacitors, J. Electroanal. Chem. 871 (2020), https://doi.org/10.1016/j.jelechem.2020.114288.
[28] K. Yu, J. Wang, X. Wang, J. Liang, C. Liang, Sustainable application of biomass by-products: Corn straw-derived porous carbon nanospheres using as anode materials for lithium ion batteries, Mater. Chem. Phys. 243 (2020), https://doi.org/10.1016/j.matchemphys.2020.122644.
[29] M.K. Singh, M. Kumar, I.S. Thakur, Proteomic characterization and schizophyllan production by Schizophyllum commune ISTL04 cultured on Leucaena leucocephala wood under submerged fermentation, Bioresour. Technol. 236 (2017) 29–36, https://doi.org/10.1016/j.biortech.2017.03.170.
[30] F. López, M.M. García, R. Yánez, R. Tapias, M. Fernández, M.J. Díaz, Leucaena species valoration for biomass and paper production in 1 and 2 year harvest, Bioresour. Technol. 99 (2008) 4846–4853, https://doi.org/10.1016/j.biortech.2007.09.048.
[31] E. Taer, F. Apriwandi, R.T. Hasanah, Nanofiber-enrich activated carbon coin derived from tofu dregs as electrode materials for supercapacitor, Commun. Sci. Technol. 6 (2021) 41–48. https://doi.org/10.21924/CST.6.1.2021.407.
[32] E. Taer, A. Apriwandi, N. Nursyafni, R. Taslim, Averrhoa bilimbi leaves-derived oxygen doped 3D-linked hierarchical porous carbon as high-quality electrode material for symmetric supercapacitor, J. Energy Storage. 52 (2022), https://doi.org/10.1016/j.est.2022.104911.
[33] S. Palisoc, J.M. Dungo, M. Natividad, Low-cost supercapacitor based on multi-walled carbon nanotubes and activated carbon derived from Moringa Oleifera fruit shells, Heliyon. 6 (2020) e03202.
[34] J. Deng, T. Xiong, H. Wang, A. Zheng, Y. Wang, Effects of cellulose, hemicellulose, and lignin on the structure and morphology of porous carbons, ACS Sustain. Chem. Eng. 4 (2016) 3750–3756, https://doi.org/10.1021/acssuschemeng.6b00388.
[35] E.E. Miller, Y. Hua, F.H. Tezel, Materials for energy storage: Review of electrode materials and methods of increasing capacitance for supercapacitors, J. Energy Storage. 20 (2018) 30–40, https://doi.org/10.1016/j.est.2018.08.009.
[36] X. Wu, L. Jiang, C. Long, Z. Fan, From flour to honeycomb-like carbon foam: Carbon makes room for high energy density supercapacitors, Nano Energy. 13 (2015) 527–536, https://doi.org/10.1016/j.nanoen.2015.03.013.
[37] E. Taer, A. Apriwandi, B.K.L. Dalimunthe, R. Taslim, A rod-like mesoporous carbon derived from agro-industrial cassava petiole waste for supercapacitor application, J. Chem. Technol. Biotechnol. 96 (2021) 662–671, https://doi.org/10.1002/jctb.6579.
[38] E. Taer, N.Y. Effendi, R. Taslim, A. Apriwandi, Interconnected micro-mesoporous carbon nanofiber derived from lemongrass for high symmetric supercapacitor performance, J. Mater. Res. Technol. 19 (2022) 4721–4732, https://doi.org/10.1016/j.jmrt.2022.06.167.
[39] M.M. Baig, I.H. Gul, Conversion of wheat husk to high surface area activated carbon for energy storage in high-performance supercapacitors, Biomass and Bioenergy. 144 (2021), https://doi.org/10.1016/j.biombioe.2020.105909.
[40] Y.M. Chang, W.T. Tsai, M.H. Li, Characterization of activated carbon prepared from chlorella-based algal residue, Bioresour. Technol. 184 (2015) 344–348, https://doi.org/10.1016/j.biortech.2014.09.131.
[41] E. Taer, A. Apriwandi, M. Krisman, R. Taslim, A. Agustino, A. Afrianda, The physical and electrochemical properties of activated carbon electrode made from pandanus tectorius, J. Phys. Conf. Ser. 1120 (2018), https://doi.org/10.1088/1742-6596/1120/1/012006.
[42] C.W. Narvaez Villarrubia, F. Soavi, C. Santoro, C. Arbizzani, A. Serov, S. Rojas-Carbonell, G. Gupta, P. Atanassov, Self-feeding paper based biofuel cell/self-powered hybrid μ-supercapacitor integrated system, Biosens. Bioelectron. 86 (2016) 459–465, https://doi.org/10.1016/j.bios.2016.06.084.
[43] X. Li, Y. Tang, J. Song, W. Yang, M. Wang, C. Zhu, W. Zhao, J. Zheng, Y. Lin, Self-supporting activated carbon/carbon nanotube/reduced graphene oxide flexible electrode for high performance supercapacitor, Carbon N. Y. 129 (2018) 236–244, https://doi.org/10.1016/j.carbon.2017.11.099.
[44] A. Apriwandi, E. Taer, R. Farma, R.N. Setiadi, E. Amiruddin, A facile approach of micro-mesopores structure binder-free coin/monolith solid design activated carbon for electrode supercapacitor, J. Energy Storage. 40 (2021), https://doi.org/10.1016/j.est.2021.102823.
[45] J. Wang, Y. Xu, M. Yan, B. Ren, X. Dong, J. Miao, L. Zhang, X. Zhao, Z. Liu, Preparation and application of biomass-based porous carbon with S, N, Zn, and Fe heteroatoms loading for use in supercapacitors, Biomass and Bioenergy. 156 (2022), https://doi.org/10.1016/j.biombioe.2021.106301.
[46] Z. Ma, B. Jiang, Q. Yuan, L. Cao, L. Liu, J. Tian, Tobacco stalks core-derived activated carbon with high capacitance by ZnCl 2 for supercapacitors, (2021) 121–126. https://doi.org/10.21595/vp.2021.22275.
[47] E. Taer, A. Apriwandi, R. Taslim, A. Agutino, D.A. Yusra, Conversion Syzygium oleana leaves biomass waste to porous activated carbon nanosheet for boosting supercapacitor performances, J. Mater. Res. Technol. 9 (2020) 13332–13340, https://doi.org/10.1016/j.jmrt.2020.09.049.
[48] E. Taer, Y. Susanti, A. Awitdrus, S. Sugianto, R. Taslim, R.N. Setiadi, S. Bahri, A. Agustino, P. Dewi, B. Kurniasih, The effect of CO2 activation temperature on the physical and electrochemical properties of activated carbon monolith from banana stem waste, AIP Conf. Proc. 1927 (2018), https://doi.org/10.1063/1.5021209.
[49] E. Taer, L. Pratiwi, W.S. Apriwandi, R.T. Mustika, Agustino, Three-dimensional pore structure of activated carbon monolithic derived from hierarchically bamboo stem for supercapacitor application, Commun. Sci. Technol. 5 (2020) 22–30, https://doi.org/10.21924/cst.5.1.2020.180.
[50] G. Wang, H. Wang, X. Lu, Y. Ling, M. Yu, T. Zhai, Y. Tong, Y. Li, Solid-state supercapacitor based on activated carbon cloths exhibits excellent rate capability, Adv. Mater. 26 (2014) 2676–2682, https://doi.org/10.1002/adma.201304756.
[51] I.I.G. Inal, S.M. Holmes, A. Banford, Z. Aktas, The performance of supercapacitor electrodes developed from chemically activated carbon produced from waste tea, Appl. Surf. Sci. 357 (2015) 696–703, https://doi.org/10.1016/j.apsusc.2015.09.067.